Physiological constraints for an intraocular inductive distance sensor

Dries Doornaert[1,*], Christ Glorieux[2], Robert Puers[3], Herbert De Gersem[1],
Werner Spileers[4], Johan Blanckaert[5]

***Abstract*— In this paper the design restrictions of an inductive sensor for an intraocular lens with focus control on the basis of a marker implanted in the ciliary muscle of the eye are discussed in the framework of anatomical and physiological influences and constraints: limitations on the marker size, influences of tissue conduction and effects of off-axis implantation of the marker with respect to the coil.**

I. Introduction

The standard treatment for cataracts disease is to extract the natural crystalline lens for the eye and replace it with an artificial intraocular lens (IOL) [16]. These IOLs come in roughly three designs: monofocal [16], multifocal [15] and accommodating [18]. The monofocal design is commonly implanted but obviously lacks focussing functionality. Multifocal lenses meet the demand of multiple focal points but a the cost of several issues such as glare [18], lowered contrast sensitivity [3], [18], [22] , halos [18] and direct light intolerance [18]. Additionally the multifocal design does not provide a complete restoration of the human accommodating system, since it only comprises a fixed number of focal points. More recently accommodating lens designs have been proposed in order to overcome the issues of multifocal lens design. The three major designs are classified as singular accommodative [17], [19], [26], piggyback [1], [2], [20], [22] and capsular refilling [23]–[25]. These designs have issues such as instability [25], inadequate accommodative power [25] and others [13], [25]. These accommodative IOLs are based on the change of focal plane position due to ciliary muscle induced movements of the lens within the capsular bag volume. Since this movement depends on the stiffness of the surrounding tissue, which increases with time [14], it is expected that over time restoration will be required.

An alternative design for an accommodative IOL is to electronically adapt the focal distance of the lens [8], [11], [12]. The system used here is based on inductively sensing the contraction state of the ciliary muscle and liquid crystal based lenses to adapt the dioptric power [8], [11]. The principle is based on a marker, implanted in the ciliary muscle, getting nearer and farther from the sensor coil due to contraction and relaxation of the ciliary muscle. The goal of this paper is to assess the magnitude of influences and constraints due to the anatomical environment around the inductive sensor and marker. A numerical study is presented that adapts this type of sensor to the dimensions and restrictions of an eye. Also results from a numerical simulation with off-axis movement of the marker, which can occur in the case of a non-ideal implant location, is included.

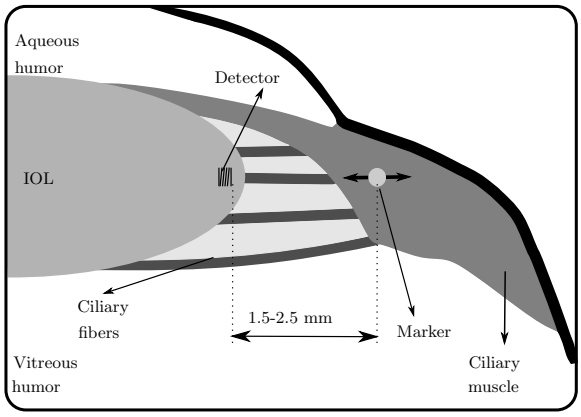

Fig. 1. Schematic representation of the inductive sensor for the intraocular lens system. A highly conductive marker is implanted in the ciliary muscle of the eye and moves when the muscle contracts or relaxes. The position of the marker has an influence on the inductance of the detection coil embedded inside the IOL. In this way the inductance is a measure for the contraction state of the ciliary muscle.

II. Concept of an inductive sensor for an electro-optic lens

An accommodative intraocular lens (IOL), has to adapt its focal length according to the demands from the visual cortex. Here the design is based on electronically adaptable lenses, which are immobilised in the capsular bag volume, thereby eliminating the influence of the time varying stiffness from the capsular bag [14]. The lenses are based on liquid crystal technology [27] and change focal distance by applying an AC-voltage across the liquid crystal volumes. Detection of the information from the visual cortex is done by optically detecting iris contraction [12] or by inductively sensing ciliary muscle contraction [8], [11]. This paper focusses on the inductive detection system. The system is based on a highly conductive marker, which is implanted into the ciliary muscle of the eye and is aligned with an inductive detection coil within the IOL [8] (Fig. 1). If the ciliary muscle contracts, the marker moves closer along the central axis of the detection coil hereby changing the inductance L of this coil and the resonance frequency f of a Colpitts

* One of the authors (D.D.) is grateful to FWO-V for financial support (PhD scholarship 2012-2016).

[1] KU Leuven - Kulak, Wave Propagation and Signal Processing Research Group
[2] Laboratory for Acoustics and Thermal Physics, Department of Physics and Astronomy, KU Leuven
[3] ESAT - MICAS, KU Leuven
[4] Department of Ophthalmology, University Hospitals Leuven
[5] UZ Leuven and Eye & Refractive Center Ieper

978-1-4244-7929-0/14/$26.00 ©2014 IEEE

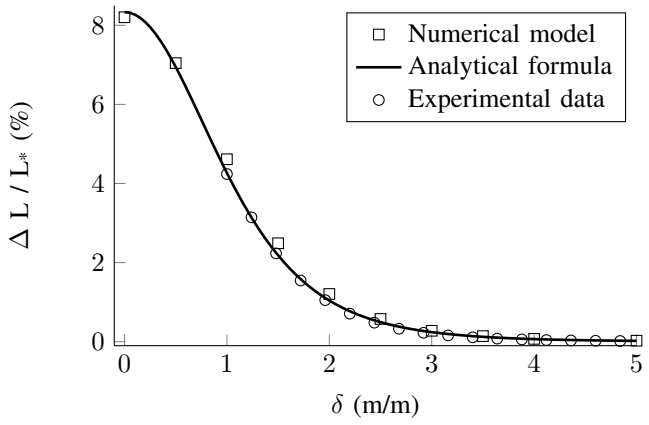

Fig. 2. Data [9] for a detection coil with radius $R = 2$ mm and marker radius $r = 1$ mm. The numerical data were generated by FEMM [21] for a vacuum setup. The analytical relation for vacuum while the experimental data were gathered for a setup in air. The experimental data, the analytical equation and the numerical model are in good correspondence.

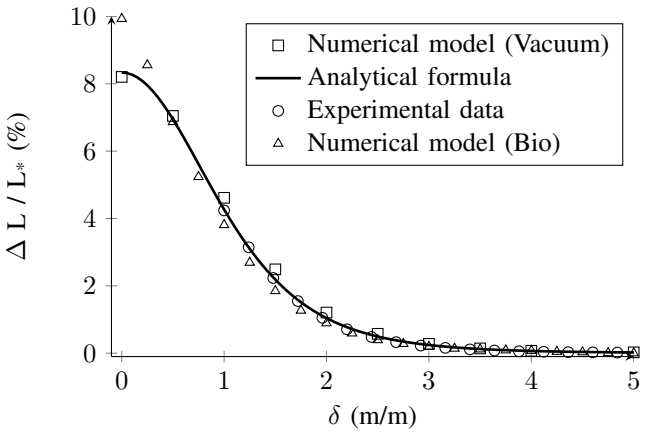

Fig. 3. Data [9] for a detection coil with radius $R = 2$ mm and marker radius $r = 1$ mm. The numerical data were generated by FEMM [21] for both a vacuum setup and a setup in biological tissue (watery environment). The analytical equation holds for vacuum while the experimental data were gathered for a setup in air. The experimental data, the analytical equation and the numerical models are in good correspondence.

oscillator circuit in which the coil is integrated [11]. This type of detector has been numerically modelled for vacuum conditions [9] with the finite-element software FEMM [21]. In [9], a theoretical model for vacuum and analysis of the modelling assumptions have been developed. This model shows that there exists a relation between the radius of the marker r, the radius of the detection coil R, the distance between the centre of the marker and the coil d and the relative change in inductance L:

$$\frac{\Delta L}{L_*} = \frac{2}{3}\frac{\mathcal{R}^3}{(\mathcal{R}^2+\delta^2)^3}, \tag{1}$$

with $\mathcal{R} = \frac{R}{r}$, $\delta = \frac{d}{r}$ and L_* the inductance when no marker is present. It has been shown that this relation also holds for an experiment in laboratory conditions (Fig. 2) [9]. Eq. 1 can be rewritten as a relative frequency shift of the oscillator signal:

$$\frac{\Delta f}{f_*} \simeq \frac{1}{3}\frac{\mathcal{R}^3}{(\mathcal{R}^2+\delta^2)^3}, \tag{2}$$

with f_* the resonance frequency of the oscillator circuit without a marker present. From this equation the maximum amplitude of a signal (i.e. contraction from a relaxed state to a fully contracted state) Δf can be calculated and compared to the noise generated in the setup.

III. Physiological constraints for the numerical models

In the previously mentioned models there were two major assumptions on which to the results for the inductive sensor were based:

1) the marker moves in a vacuum or air environment,
2) the marker moves perfectly along the central axis of the detection coil.

In addition, no restriction was set on the size of the markers although it is clear that not all sizes are suitable for implantation in a human eye.

A. Biological tissue

The numerical simulations for the inductive sensor [9] (Fig: 2) were performed with the assumptions of a vacuum medium and a marker, which is a perfect electric conductor. When the inductive sensor is applied for intraocular lenses the medium between the marker and the detection coil will be biological tissue instead of vacuum. Biological tissue has a finite non zero electrical conductivity σ and high relative permittivity ϵ_r, which influences the behaviour of oscillating electromagnetic fields at a certain frequency. Both σ and ϵ_r have a high frequency dispersion [10]. In the application of an intraocular sensor a frequency f in the order of 10 MHz is applied giving $\sigma \simeq 1$ S/m and $\epsilon_r \simeq 70$ [10], [29]. Since $2\pi f\epsilon \ll \sigma$ the displacement current can be ignored allowing for quasi-magnetostatic calculations. If the conductivity of the medium is taken into account for the numerical FEMM model also the marker needs to be modelled as a realistic material, gold, with a finite electrical conductivity $\sigma_{marker} \simeq 40$MS/m. The same dimensional modelling parameters as applied for Fig. 2 are used: an axially symmetric cylindrical coil with height $h = 0.42$ mm, thickness $t = 0.21$ mm, radius $R = 2$mm and number of turns $N = 1$, which is enclosed in a fixed modelling sphere with radius $k = 20$ mm together with a spherical marker with radius $r = 1$mm placed at a distance d from the face of the coil [9]. There is a substantial influence (Fig. 3) of the magnitude of the conductivity when the marker is very close to the coil. At relative distance larger than $\delta = 0.5$ the correspondence between the numerical model for vacuum, the analytical model, the experiment and the numerical model for biological tissue are in good correspondence.

B. Size limitations and range

In a natural human eye the crystalline lens is suspended via ciliary fibers to the ciliary muscle. On average the radius of

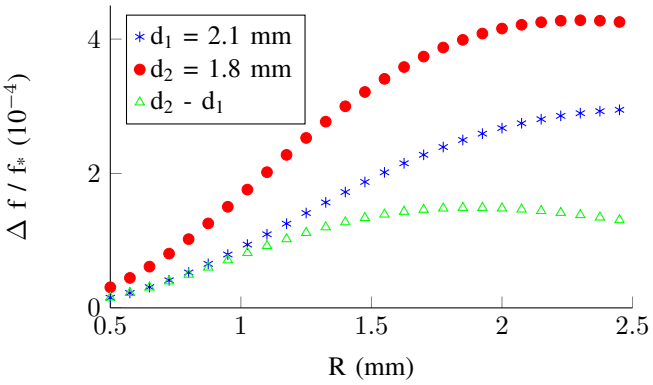

(a) Calculated relative frequency response of a marker implanted in the natural, unstretched, capsular bag. The optimum response lies around $R = 1.8$ mm and requires the possibility to at least measure a relative frequency shift of 10^{-4}.

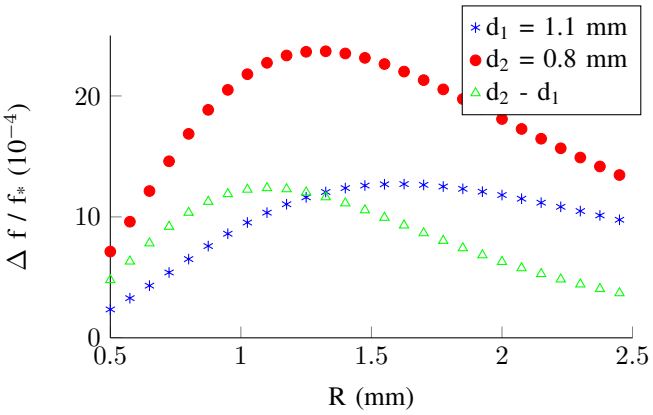

(b) Calculated relative frequency response of a marker implanted in a capsular bag with a radius stretched over 1 mm. The optimum response lies around $R = 1$ mm and requires the possibility to at least measure a relative frequency shift of 10^{-3}.

Fig. 4. Numerical model (Eq. 2) of a marker with radius $r = 0.5$mm implanted in the ciliary muscle at a distance d from the detection coil with radius R. The dots represent a relaxed ciliary muscle state, the stars represent an accommodated ciliary muscle state, the triangles depict the differences between the dots and stars. Stretching the capsular bag and thus shortening the distance between the detection coil and the marker leads to smaller detection coil radii and higher measurement accuracy.

the ciliary muscle in relaxed state (0 Diopter [D]) is 6.7 mm while the average radius of the relaxed lens (0 D) is 4.6 mm. In contracted state (8 D) the average ciliary muscle radius is 6.4 mm and the average radius of the lens is 4.4 mm [4]–[6], [30], [31]. Without stretching the capsular bag beyond its natural limits the distance between the lens and the ciliary muscle is 1.8 mm in the accommodated state and 2.1 mm in the relaxed state (Tab. I). In order to precisely monitor the state of contraction of the ciliary muscle so that the dioptric strength can be precisely and smoothly adapted, the sensor should be able to resolve a fraction of the maximum 0.3 mm change in marker position at a maximum distance of 2.1 mm. The capsular bag could also be stretched to reduce this distance [32].

The implanted marker size is limited to a radius of approximately $r = 0.5$ mm in order to fit in the ciliary muscle [28]. The radius of the detection coil is at most $R = 2$ mm since it has to fit inside the capsular bag volume and has to be placed near the edge. Using Eq. 2 the resolution of the

Ciliary muscle radius (mm)		Lens radius (mm)	
0D	8D	0D	8D
6.7	6.4	4.6	4.4
Difference between the ciliary muscle and the lens radii (mm)			
0D - 0D	0D - 8D	8D - 0D	8D - 8D
2.1	2.3	1.8	2.2

TABLE I

VALUES FOR THE CILIARY MUSCLE AND CRYSTALLINE LENS RADII (MM) WITHOUT ACCOMMODATION (0 DIOPTER [D]) AND FULL ACCOMMODATION (8D). THE DIFFERENCE BETWEEN LENS AND CILIARY MUSCLE DIAMETER GIVES AN ESTIMATE FOR THE MINIMUM RANGE AN INDUCTIVE SENSOR NEEDS TO HAVE IN ORDER TO DETECT CILIARY MUSCLE MOVEMENTS WITH A DETECTION COIL PLACED INSIDE THE LENS.

sensor given the restrictions is estimated (Fig. 4). Without stretching the capsular bag, a minimum relative measurement accuracy of 10^{-4} is needed to detect full accommodation (0D to 8D). With a stretched capsular bag on the other hand a minimum accuracy of only 10^{-3} is needed. With our current experimental test system, the typical relative experimental noise level on the marker-coil distance is $\frac{2\text{kHz}}{8\text{MHz}} \simeq 2 \cdot 10^{-4}$, which satisfies this requirement. Also, when the capsular bag is stretched, the optimum radius of the detection coil shifts to smaller radii making it more convenient to implant.

C. Off-axis movement

The numerical simulations for the inductive sensor [9] (Fig: 2, 3) were performed with the assumption of axial movement with respect to the central coil axis. This assumption will not hold for an implanted lens since it is not straightforward to maintain millimeter precision when surgically implanting the marker. If the relation between off-axis movements and the coil inductance and oscillation frequency is monotonic, then the accommodation software can be calibrated to properly incorporate the effect. The effect has been numerically modelled (Fig. 5) using 3D electromagnetic field simulation by CST EM Studio [7] and by assuming a marker that moves away from the detection coil with a fixed angle with respect to the central axis of the coil. Moving at an angle turns out to be beneficial for the close range sensitivity of the sensor. This is however irrelevant for the application of an intraocular lens sensor. The reason for the higher $\frac{\Delta L}{L_*}$ is that due to the finite size of the coil, the marker will still be directly above the coil surface during the first steps. This means that in moving a larger distance the marker has moved a smaller distance away from the coil surface. At larger distances $d > 1$mm the effect of moving at an angle is much smaller.

IV. CONCLUSION

The design for an accommodative lens using opto-electronical control needs information on the dioptric strength desired by the visual cortex. An inductive sensor detecting the position of a highly conductive marker implanted in the ciliary muscle gives a possibility to monitor its state of contraction, which is a reliable indicator of the desired dioptric strength. Three issues that should be taken into account in the design of this sensor, i.e. the

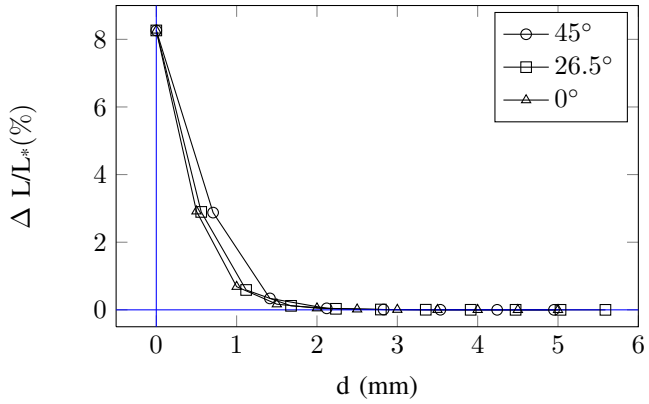

Fig. 5. Data for off-axis movement of a marker modelled via CST EM Studio [7]. A marker ($r = 0.5$mm) moves away from the centre of the detection coil ($R = 1$mm) under a fixed angle (45°,26.5°,0°) with the central axis of the coil. For $d > 1$mm there is no significant difference, for $d < 1$mm moving under an angle gives a higher response than moving along the central axis of the detection coil.

sensor range, vacuum vs. biological and on- or off-axis movement, were discussed. It was shown that the range of the sensor is sufficient to use natural dimensions for the artificial lens, it would however be beneficial to stretch the capsular bag to a higher radius. Models showed that the biological tissue in first approximation will not influence the sensor's functionality. Modelling off-axis movement resulted in apparent close range enhanced sensitivity but this effect is mainly attributed to the coil size and modelling assumptions. Overall, there are no significant limitations or deteriorating effects of the investigated parameters on the functionality of the sensor.

REFERENCES

[1] David J Apple, Marcela Escobar-Gomez, Brian Zaugg, Guy Kleinmann, and Andreas F Borkenstein. Modern cataract surgery: unfinished business and unanswered questions. *Survey of ophthalmology*, 56(6 Suppl):S3–53, 2011.

[2] José M Artigas, Adelina Felipe, Manuel Diaz-Llopis, Salvador Garcia-Delpech, and Amparo Navea. Imaging quality of bifocal piggyback intraocular lens versus ReSTOR and TECNIS multifocal lenses. *European journal of ophthalmology*, 20(1):71–5, 2010.

[3] Penny a Asbell, Ivo Dualan, Joel Mindel, Dan Brocks, Mehdi Ahmad, and Seth Epstein. Age-related cataract. *Lancet*, 365(9459):599–609, 2005.

[4] N Brown. The change in shape and internal form of the lens of the eye on accommodation. *Experimental eye research*, 15(4):441–59, April 1973.

[5] N Brown. The change in lens curvature with age. *Experimental eye research*, 19(2):175–83, August 1974.

[6] H J Burd, S J Judge, and J a Cross. Numerical modelling of the accommodating lens. *Vision research*, 42(18):2235–251, August 2002.

[7] CST - Computer Simulation Technology. CST studio suite 2013, 2013.

[8] Dries Doornaert, Christ Glorieux, Herbert De Gersem, Robert Puers, Werner Spileers, and Johan Blanckaert. Intraocular electro-optic lens with ciliary muscle controlled accommodation. *Conference proceedings : ... Annual International Conference of the IEEE Engineering in Medicine and Biology Society. IEEE Engineering in Medicine and Biology Society. Conference*, 2013:3190–3, July 2013.

[9] Dries Doornaert, Christ Glorieux, Herbert De Gersem, Robert Puers, Werner Spileers, and Johan Blanckaert. Distance measurement by inductive sensing of a marker for an implantable intraocular lens. *Submitted to: Sensors and actuators A*, 2014.

[10] S Gabriel, R W Lau, and C Gabriel. The dielectric properties of biological tissues: II. Measurements in the frequency range 10 Hz to 20 GHz. *Physics in medicine and biology*, 41(11):2251–69, November 1996.

[11] Christ Glorieux, Johan Blanckaert, and Robert Puers. Bionic eye lens PCT/BE2011/000045, 2006.

[12] Elenza Inc. electronic Intraocular Lens. http://elenza.com/, 2012.

[13] Jorge Cazal, Cosme Lavin-Dapena, Jesus Marin, Carlos Vergés, Jorge Cazal, Cosme Lavin-Dapena, Jesus Marín, and Carlos Vergés. Accommodative Intraocular Lens Tilting. *American Journal of Ophtalmology*, 140(2):341–344, August 2005.

[14] S. Krag. Mechanical Properties of the Human Posterior Lens Capsule. *Investigative Ophthalmology & Visual Science*, 44(2):691–696, February 2003.

[15] Martin Leyland and Edoardo Zinicola. Multifocal versus monofocal intraocular lenses in cataract surgery: a systematic review. *Ophthalmology*, 110(9):1789–98, September 2003.

[16] E J Linebarger, D R Hardten, G K Shah, and R L Lindstrom. Phacoemulsification and modern cataract surgery. *Survey of Ophthalmology*, 44(2):123–147, 1999.

[17] Marian S Macsai, Lissa Padnick-Silver, Bruno M Fontes, Marian S. Macsai, Lissa Padnick-Silver, and Bruno M. Fonte. Visual outcomes after accommodating intraocular lens implantation. *Journal of Cataract & Refractive Surgery*, 32(4):628–633, April 2006.

[18] Nick Mamalis. Accommodating intraocular lenses. *Journal of Cataract & Refractive Surgery*, 30(12):2455–2456, December 2004.

[19] Leonardo Mastropasqua, Lisa Toto, Mario Nubile, Gennaro Falconio, and Enzo Ballone. Clinical study of the 1CU accommodating intraocular lens. *Journal of Cataract & Refractive Surgery*, 29(7):1307–1312, July 2003.

[20] Stephen D McLeod, Luis G Vargas, Val Portney, and Albert Ting. Synchrony dual-optic accommodating intraocular lens: Part 1: Optical and biomechanical principles and design considerations. *Journal of Cataract & Refractive Surgery*, 33(1):37–46, January 2007.

[21] David Meeker. femm 4.2 - www.femm.info, 2013.

[22] R Menapace, O Findl, K Kriechbaum, Ch Leydolt-Koeppl, R. Menapace, O. Findl, K. Kriechbaum, and Ch. Leydolt-Koeppl. Accommodating intraocular lenses: a critical review of present and future concepts. *Graefe's archive for clinical and experimental ophthalmology = Albrecht von Graefes Archiv für klinische und experimentelle Ophthalmologie*, 245(4):473–89, April 2007.

[23] O Nishi, T Hara, Y Sakka, F Hayashi, K Nakamae, and Y Yamada. Refilling the lens with a inflatable endocapsular balloon: surgical procedure in animal eyes. *Graefe's archive for clinical and experimental ophthalmology = Albrecht von Graefes Archiv für klinische und experimentelle Ophthalmologie*, 230(1):47–55, January 1992.

[24] Okihiro Nishi, Kayo Nishi, Yutaro Nishi, and Shiao Chang. Capsular bag refilling using a new accommodating intraocular lens. *Journal of cataract and refractive surgery*, 34(2):302–9, February 2008.

[25] Yutaro Nishi, Kamiar Mireskandari, Peng Khaw, and Oliver Findl. Lens refilling to restore accommodation. *Journal of Cataract & Refractive Surgery*, 35(2):374–382, February 2009.

[26] Donald R Sanders and Monica L Sanders. Visual performance results after Tetraflex accommodating intraocular lens implantation. *Ophthalmology*, 114(9):1679–84, September 2007.

[27] Susumu Sato. Applications of Liquid Crystals to Variable-Focusing Lenses. *Optical Review*, 6(6):471–485, 1999.

[28] Amy L Sheppard and Leon N Davies. The effect of ageing on in vivo human ciliary muscle morphology and contractility. *Investigative ophthalmology & visual science*, 52(3):1809–16, March 2011.

[29] V Spitzer, M J Ackerman, a L Scherzinger, and D Whitlock. The visible human male: a technical report. *Journal of the American Medical Informatics Association : JAMIA*, 3(2):118–30, 1996.

[30] S a Strenk, J L Semmlow, L M Strenk, P Munoz, J Gronlund-Jacob, and J K DeMarco. Age-related changes in human ciliary muscle and lens: a magnetic resonance imaging study. *Investigative ophthalmology & visual science*, 40(6):1162–1169, May 1999.

[31] SA Strenk, LM Strenk, and S Guo. Magnetic resonance imaging of aging, accommodating, phakic, and pseudophakic ciliary muscle diameters. *Journal of Cataract & Refractive Surgery*, 32(11):1792–1798, 2006.

[32] Noël M Ziebarth, David Borja, Esdras Arrieta, Mohamed Aly, Fabrice Manns, Isabelle Dortonne, Derek Nankivil, Rakhi Jain, and Jean-Marie Parel. Role of the lens capsule on the mechanical accommodative response in a lens stretcher. *Investigative ophthalmology & visual science*, 49(10):4490–6, October 2008.